Investigating the Heaviest Halogen: Lessons Learned from Modeling the Electronic Structure of Astatine's Small Molecules

Vincent T. Casetti,† James MacLean,† Adam D. Ayoub,† Rain J. Fredericks,‡
Jacob A. Adamski,¶ and Alexander A. Rusakov*,†

†*Department of Chemistry, Oakland University, Rochester, Michigan, 48309 USA*
‡*Material Science and Engineering Department, University of Michigan, Ann Arbor, Michigan, 48109 USA*
¶*Department of Chemistry, University of Michigan, Ann Arbor, Michigan, 48109 USA*

E-mail: rusakov@oakland.edu
Phone: +1 (248) 370 2333

Abstract

We present a systematic study of electron-correlation and relativistic effects in diatomic molecular species of the heaviest halogen astatine (At) within relativistic single- and multi-reference coupled-cluster approaches and relativistic density functional theory. We establish revised reference *ab initio* data for the ground states of At_2, HAt, AtAu, and AtO^+ using a highly accurate relativistic effective core potential model and in-house basis sets developed for accurate modeling of molecules with large spin-orbit effects. Spin-dependent relativistic effects on chemical bonding in the ground state are comparable to the binding energy or even exceed it in At_2. Electron-correlation effects near the equilibrium internuclear separation are mostly dynamical and can be adequately captured using single-reference CCSD(T). However, bond elongation in At_2 and, especially, AtO^+ results in rapid manifestation of its multi-reference character. While useful for evaluating the spin-orbit effects on the ground-state bonding and properties, the two-component density functional theory lacks predictive power, especially in combination with popular empirically adjusted exchange-correlation functionals. This drawback supports the necessity to develop new functionals for reliable quantum-chemical models of heavy-element compounds with strong relativistic effects.

1 Introduction

Apart from superheavy elements, the rarest naturally occurring element and the heaviest halogen astatine ${}_{85}$At remains one of the most “enigmatic” in the periodic table.[1,2] The ^{211}At isotope's unique properties have been attracting much attention in the nuclear medicine community for several decades. As a pure α-emitter, ^{211}At is ideally suited for targeted therapy of malignant tumors due to its half-life, linear energy transfer, and the absence of harmful radioactive or toxic decay products or harmful deceleration γ-rays.[3–6] However, ^{211}At's scarcity due to production complexity and cost keeps its experimental chemistry elusive, thus creating a major obstacle in translating accelerator-generated elemental ^{211}At to radiopharmaceuticals.[7]

The absence of spectroscopic data even for diatomic species, such as At_2, HAt, or AtO^+, leaves state-of-the-art *ab initio* quantum-chemical calculations the sole source of basic reference data on the equilibrium internuclear distance R_e, dissociation energy D_e, and vibrational frequency ω_e. As a heavy element, astatine exhibits strong relativistic effects that extend to its valence electrons. The spin-orbit interaction causes substantial energetic and spatial differences[8] within $5p_{1/2}$–$5p_{3/2}$, $5d_{3/2}$–$5d_{5/2}$, and $6p_{1/2}$–$6p_{3/2}$ shells, thereby affecting correlations of the subvalence and valence electrons, which results in a potential departure of the astatine's chemical behavior from other halogens. Methodological complexities of treating the interplay of relativistic and correlation effects lead to substantially varying predictions even across recent advanced models. For example, the CCSD(T) version of a two-component relativistic coupled-cluster calculation (2c-CCSD(T)) of At_2 in Ref. 9 with the X2C Hamiltonian and the complete basis set (CBS) extrapolation across Dyall's acv$X$z ($X = 2, 3, 4$) correlates 5d-, 6s-, and 6p-electrons and yields $D_e(At_2)= 0.791$ eV. The authors of Ref. 9 mention insignificant differences between single-reference CCSD and multi-reference Fock-space CCSD (FS CCSD) results, albeit without giving specific numbers, and judge in favor of 2c-CCSD(T) as the method of choice. Using a similar argument, the authors of Ref. 10 conclude that the 0_g^+ ground state of At_2 is predominantly single-reference as their multi-reference configuration interaction MRCISD+Q results (R_e=3.046 Å, D_e=0.68 eV) agree with earlier four-component (4c-) CCSD(T) calculations (R_e=3.046 Å, D_e=0.63 eV).[11] Finally, all-electron calculations combining valence-only CBS-extrapolated scalar relativistic CCSD(T) data with 4c-CCSD(T)/av3z spin-orbit corrections in Ref. 12 predict R_e=2.986 Å and D_e=0.854 eV. Thus, D_e predictions based on relativistic coupled-cluster approaches fall within the range of *ca.* 0.22 eV, or 5 kcal/mol. Similarly, suitable relativistic CCSD(T) calculations for the HAt molecule yield D_e predictions of 2.281[11] and 2.485[12] eV, also allowing for a *ca.* 5 kcal/mol uncertainty window. Assuming that At_2 is a relatively weakly bonded molecule with $D_e < 20$ kcal/mol, a 5 kcal/mol uncertainty across seemingly high-level relativistic quantum-chemical results is disconcerting and calls for further scrutiny of the appropriate *ab initio* methodologies.

A seminal publication by Sergentu *et al.*[13] puts to the test conventional quantum-chemical recipes based on Density Functional Theory (DFT) to describe or predict the chemical behavior at the bottom of the periodic table using small molecules and molecular ions of astatine At_2, HAt, AtF_3, and AtO^+ as a case in point. While several popular exchange-correlation functional (XCF) approximations such as B3LYP,[14] PBE0,[15,16] or HSE06[17–19] display reasonable behavior, the authors do not assess their reliability for bond strengths and recognize a gap in the DFT development for heavy-element chemistry. To complicate matters even further, a recent article by Aebersold and Wilson[20] demonstrates that for heavy-element molecules from the An66 database modeled with spin-orbit relativistic density functional theory (RDFT), errors from the standard basis set families are comparable to those from XCFs. The entanglement of these two major sources of errors renders the quality of spin-orbit RDFT models too chaotic to propose reasonable computational recipes.

The objective of this article is threefold. First, we establish new high-level *ab initio* reference data for diatomic At species. Second, we analyze potential multi-reference effects and spin-orbit–correlation interference. Third, based on the new *ab initio* results, we assess several common relativistic DFT approaches and delineate the role of XCF approximations from basis set errors. In addition to the previously mentioned At_2 and HAt, we investigate the AuAt molecule and AtO^+ molecular ion. Astatine–gold interactions attract attention due to the growing interest in gold clusters as At carriers in new therapeutic strategies.[21,22] Also, At may bear chemical similarities to the superheavy element nihonium ($_{113}$Nh) and serve as a model system to calibrate thermochromatographic experiments on Nh identification and characterization based on its interaction with a gold surface.[23,24] Finally, the AtO^+ molecular cation's chemistry plays a key role in understanding astatine's behavior in common solvents.[25,26]

2 Computational details

2.1 Effective core potentials and basis sets

The focus on chemical properties justifies the replacement of At and Au core electrons with relativistic effective core potentials (RECPs). In this work, we use accurate small-core shape-consistent RECPs[27] (available on the Petersburg Nuclear Physics Institute Quantum Chemistry Laboratory website[28]). Optimized for valence shells, these RECPs also offer a reasonable accuracy in describing outer-core–valence correlations involving 5*s*-, 5*p*-, and 5*d*-shells of At and Au atoms. With RECPs replacing 60 core electrons, we treat the remaining 25 At and 19 Au atoms' electrons explicitly.

To extrapolate the results of correlated wavefunction calculations to the complete basis set (CBS) limit, we develop triple-, quadruple-, and quintuple-ζ (respectively, TZ, QZ, and 5Z) correlation-consistent basis sets tailored for the chosen RECP model. Our correlation-consistent basis sets are an adaptation and extension of those accompanying Stuttgart–Cologne energy-adjusted RECPs.[29,30] For both At and Au, we start with the primitive Gaussian exponents already optimized for the cc-CVnZ-PP[31,32] families of basis sets. Modifications apply to the contracted s-, p-, and d-functions to account for a different functional form of the RECP operator. In particular, such modifications are necessary for the basis sets to reflect the effects of spin-orbit interaction.[33–35] To this end, we decontract the original functions and perform two-component spin-orbit Hartree–Fock calculations for atomic (or ionic) species. These calculations result in atomic spinors, *i.e.*, two-component and generally complex extensions of the usual atomic orbitals, whose coefficients we then use to create new contracted basis functions. The resulting basis sets feature different contractions for $p_{1/2}$ and $p_{3/2}$, as well as $d_{3/2}$ and $d_{5/2}$ functions, reflecting the spatial difference between spin–orbit-split p- and d-shells. We do not modify the original sets' uncontracted core-valence correlation functions, polarization, or diffuse Gaussian exponents.

For astatine basis sets, it is convenient to create all $5s_{1/2}$, $5p_{1/2}$, $5p_{3/2}$, $5d_{3/2}$, $5d_{5/2}$, $6s_{1/2}$, $6p_{1/2}$, and $6p_{3/2}$ contracted functions based on the two-component Hartree–Fock calculations for a closed-shell anion At$^-$. Working with the open-shell solution for an At atom is more complicated and results in a virtually indistinguishable basis set. The situation with gold is somewhat cumbersome due to a narrower $5d_{5/2}$–$6s_{1/2}$ energy gap and the presence of low-lying $6p_{1/2}$ and $6p_{3/2}$ virtual spinors. As advised in Ref. 31, it is necessary to derive flexible basis sets from $5d^{10}6s^1$, $5d^9 6s^2$, and $5d^8 6s^2 6p^1$ atomic states. To this end, we implement the following scheme. Core-like $5s_{1/2}$, $5p_{1/2}$, and $5p_{3/2}$ contracted functions represent the corresponding Hartree–Fock spinors for Au$^+$. To derive sub-valence $5d_{3/2}$ and $5d_{5/2}$ and valence $6s_{1/2}$ spinors, we use an average-of-configuration open-shell Au^0 solution that covers $5d^{10}6s^1$ and $5d^9 6s^2$ atomic states. Finally, $6p_{1/2}$ and $6p_{3/2}$ contractions result from the average-of-configuration open-shell Au^0 solution for the $5d^8 6s^2 6p^1$ state. We calculate all these solutions using the DIRAC19[36] implementation of the relativistic 2c-Hartree–Fock method with the RECP Hamiltonian.[37]

The CBS limit extrapolation procedure in DFT, unlike wavefunction correlated methods, is not well-established.[38] To approach the CBS limit in RDFT calculations, we develop an adaptation of the universal Gaussian basis set (UGBS).[39] Our modifications include the removal of core-like exponents for heavy atoms with RECPs, adding extra polarization functions, and further augmentation. Without universally accepted basis sets for RDFT calculations, our modified UGBS approach attains sufficient flexibility without developing numerical instabilities, at least for small systems. The systematic development of optimal basis sets for RDFT calculations is beyond the scope of this article. The parameters of all basis sets developed for correlated wavefunction and RDFT calculations are given in the Supporting Information.

2.2 Relativistic coupled-cluster calculations

We perform scalar one-component (1c-) and spin-orbit two-component (2c-) single-reference CCSD(T) simulations using the DIRAC19 program.[36] For At and Au, we employ aug-cc-pwCVnZ-PP ($n = 3$–5) basis sets modified for spin-orbit calculations with shape-consistent RECPs, as described in Sec. 2.1, while for H and O we use the original aug-cc-pVnZ and aug-cc-pwCVnZ ($n = 3$–5)[40–43] sets, respectively. To incorporate outer-core–valence correlation effects involving $5s$-, $5p_{1/2}$–$5p_{3/2}$-, and, especially, $5d_{3/2}$–$5d_{5/2}$-shells we keep all 25 electrons of At and 19 electrons of Au outside of the RECPs' small cores active. We find it possible to ignore excitations to virtual spinors with energies above 60 hartree with impunity, thus avoiding unnecessarily time-consuming computations for large basis sets. We evaluate single-reference coupled-cluster binding energies against the sum of individual atomic (or ionic for AtO^+) energies. For the CBS extrapolation, we apply Eq. 2 from Ref. 12, $E_n = E_{CBS} + \frac{B}{(n+1/2)^4}$.

A noteworthy caveat of 2c-CCSD(T) calculations for At_2 in DIRAC19 is generating the ground-state 2c-Hartree–Fock reference. Similar to I_2,[44] a plain Kramers-restricted 2c-Hartree–Fock calculation for At_2 converges to a spurious excited state, leading, in turn, to an equally spurious 2c-CCSD(T) solution. Using the 2c-Hartree–Fock solution for At_2^{2-} at a large R(At—At) as the guess drives the self-consistent procedure for At_2 to the actual ground state at internuclear separations around R_e. As noted by one of the manuscript's Reviewers, an alternative approach is to start the 2c calculation from a 1c solution converged at the given R value. We confirm that this method solves the convergence issue equally well. For technical details, we refer readers to Sec. S1 of the Supporting Information. Other cases do not seem to suffer from this problem.

Due to substantial bond lengths in At compounds (about 3 Å in At_2), their ground states may display some multi-reference character already near equilibrium. We perform multi-reference calculations within the relativistic Fock-space CCSD (FS CCSD) method as implemented in the EXP-T program,[45,46] which we choose for its robust dynamic denominator-shifting technique. We take closed-shell systems of At_2^{2-}, HAt^{2-}, $AuAt^{2-}$, and AtO^- to generate vacuum states and solve the FS CCSD equations in the $(0h, 0p)$, $(1h, 0p)$, and $(2h, 0p)$ Fock-space sectors, the last one corresponding to neutral At_2, HAt, AuAt, and cationic AtO^+. At dissociation, free At, Au, and H atoms emerge via creating a "hole" in closed $6p^6$, $5d^{10}6s^2$, and $1s^2$ shells, respectively. To create the corresponding model spaces for At_2, HAt, and AuAt, we use 12, 8, and 18 active holes in the $(1h, 0p)$ and $(2h, 0p)$ sectors. The energy denominator shifting technique allows the FS CCSD procedure to converge in difficult cases. We keep the denominator shifts as small as possible to facilitate convergence without compromising separability. This FS CCSD scheme can describe the atomization of At_2, HAt, and AuAt correctly, allowing us to calculate bond strengths relative to the molecular energies at large (20 bohr) internuclear separations. We describe the issues with the AtO^+ case separately in Sec. 3.4. We include spin-orbit interaction in all FS CCSD calculations.

2.3 Relativistic density functional theory calculations

We perform 2c-RDFT calculations using the collinear spin-orbit formalism[47] as implemented in the NWChem[48] program or the non-collinear[49–51] one available in the TURBOMOLE[52] suite. By design, the non-collinear approach is invariant with respect to the molecule's orientation, albeit at a higher computational cost than the collinear approximation. The magnitude of the spin-orbit interaction in Au or At is not enough to cause a significant dependence of the molecular energy on the quantization axis choice in the collinear approach and in well-behaved cases such as At_2 or HAt, both versions of 2c-RDFT yield identical results. We find AtAu simulations difficult to converge with the collinear method and rely on the TURBOMOLE non-collinear 2c-RDFT approach. Additionally, we use TURBOMOLE's 2c-RDFT for simulations with range-separated XCFs due to more efficient implementation and a wider range of available functionals.

Our reference RDFT calculations employ the PBE0[15,16] XCF approximation, which is (almost) free of empirically fitted parameters and has already demonstrated its reliability in heavy- and superheavy-element molecular modeling.[23,24,53,54] Based on the R_e for each molecule, we generate a set of internuclear separations to model the potential energy surface within a ± 0.5 Å range of R_e with a 0.1 Å step. We also utilize these grids for scanning the energy curves with coupled-cluster and RDFT methods. The molecular cation AtO^+ being a potentially more difficult case, we describe the details separately in Sec. 3.4.

We simulate the binding energy curves and compute the ground-state spectroscopic constants R_e, D_e, and ω_e using the following representatives of the main XCF families: generalized-gradient approximation (GGA) Becke-88–Perdew-86,[55–57] meta-GGAs TPSS[58,59] and SCAN,[60] global hybrids PBE0,[15,16] B3LYP,[14] TPSSh,[61] PW6B95,[62] and M06-2X,[63] and range-separated hybrids HSE06[17–19] and ωB97X-D.[64]

2.4 Composite approach

We generally follow the Feller–Peterson–Dixon approach[12,65] that treats electron-correlation effects calculated within a scalar-relativistic approximation and spin-orbit effects on molecular properties as additive.[54,65–67] In particular, we are interested in approximating 2c-CCSD(T) binding-energy E_b profiles using 1c-CCSD(T) and the geometry-dependent spin-orbit contribution $\Delta\mathrm{SO}(E_b)$ to the binding energy from RDFT. The formal expression for the composite binding energy of a diatomic molecule AB is

$$E_b(\mathrm{AB}) = E_{\mathrm{1c-CCSD(T)}}(\mathrm{AB}) - \big(E_{\mathrm{1c-CCSD(T)}}(\mathrm{A}) + E_{\mathrm{1c-CCSD(T)}}(\mathrm{B})\big) + \Delta\mathrm{SO}(E_b), \tag{1}$$

where

$$\begin{aligned}\Delta\mathrm{SO}(E_b) = {} & E_{\mathrm{2c-RDFT}}(\mathrm{AB}) - (E_{\mathrm{2c-RDFT}}(\mathrm{A}) + E_{\mathrm{2c-RDFT}}(\mathrm{B})) - \\ & - \left[E_{\mathrm{1c-RDFT}}(\mathrm{AB}) - (E_{\mathrm{1c-RDFT}}(\mathrm{A}) + E_{\mathrm{1c-RDFT}}(\mathrm{B}))\right].\end{aligned} \tag{2}$$

1c-RDFT calculations are performed without the spin-orbit RECP operator and are operationally equivalent to non-relativistic DFT.

3 Results and discussion

3.1 At_2

We summarize the equilibrium properties of the At_2 molecule in Table 1. Additionally, we present the binding energy E_b profiles near equilibrium (Fig. 1), the spin-orbit RDFT contributions $\Delta\mathrm{SO}(E_b)$ to the binding energy as a function of the bond length (Fig. 2), and juxtapose 1c-CCSD(T), 2c-CCSD(T), and Feller–Peterson–Dixon-style composite profiles combining 1c-CCSD(T) with the RDFT $\Delta\mathrm{SO}(E_b)$ contribution (Fig. 3).

Our 1c-CCSD(T) scalar relativistic results for R_e, D_e, and ω_e closely reproduce those from the most recent all-electron calculations by Vasiliu, Peterson, and Dixon[12] and corroborate the "chemical accuracy" preservation within the chosen RECP model.[27]

Our relativistic 2c-CCSD(T) results agree with the CBS-extrapolated all-electron X2C CCSD(T) ones[9] and support the reliability of the RECP model[27] for treating spin-dependent relativistic effects on valence and outer-core electrons. Although this RECP model does not include the Breit or Gaunt terms for astatine, those cannot affect its valence properties meaningfully. For instance, the mean-field Breit effects on astatine's first ionization potential and electron affinity are, respectively, 0.001[68] and 0.003 eV.[69] Apart from the Hamiltonian model, small differences likely arise from the CBS extrapolation scheme and the correlations of 5*s*- and 5*p*-electrons included in this work. We observe, for example, that the TZ-to-QZ extrapolation lowers D_e by about 0.005 eV compared to the QZ-to-5Z scheme. In contrast, the inclusion of 5*s*- and 5*p*-electrons in the correlated calculation strengthens the bond by about 0.003 eV. The magnitude of all these effects is below the "chemical accuracy" threshold of 1 kcal/mol. All At_2 coupled-cluster data presented here correspond to the QZ-to-5Z CBS extrapolation scheme.

Several sources[9,10,13] claim an essentially single-reference character of the At_2 electronic ground state. Our relativistic FS CCSD calculations aim to test this hypothesis directly and revise the underlying logic in Refs. 9,10,13. The authors of Ref. 9 suggest that single-reference CCSD and multi-reference FS CCSD results are in close agreement. This statement contradicts our findings. In particular, we find that at its respective $R_e = 2.930$ Å, single-reference 2c-CCSD predicts $D_e = 0.551$ eV, almost 30% smaller than our FS CCSD value. In Ref. 10, the authors make a stronger argument in favor of the single-reference ground state based on the agreement between their MRCISD+Q results for R_e, D_e, and ω_e and the corresponding values in Ref. 70 obtained within the 4c-CCSD(T) formalism. However, the authors of Ref. 10 indicate that they use the same basis set as in Ref. 70, although the former (aug-cc-PVTZ), unlike the one in Ref. 70, has an extra set of diffuse functions. Also, Visscher *et al.* revisited[10] their earlier results[70] to account for substantial correlation effects involving 5*d*-electrons. While multi-reference relativistic FS CCSD yields $D_e = 0.780$ eV, which is very close to the single-reference 2c-CCSD(T) result (0.777 eV), it predicts an R_e noticeably shorter by 0.1 Å, a larger ω_e, and a somewhat different shape of the E_b profile (see Table 1 and Fig. 1).

We find that for At_2, orbital-relaxation terms, or diagrams with a pair of identical "spectator" lines, dominate in the $\hat{S}_2$ operator in the $(1h, 0p)$ sector but not in $(2h, 0p)$. While orbital relaxations can be significant in FS CCSD calculations, the non-dominant role of diagrams with spectator lines in the $(2h, 0p)$ sector's $\hat{S}_2$ operator indicates the important role of double excitations in the $(2h, 0p)$ sector beyond orbital-relaxation effects. Furthermore, we observe that the determinant that is responsible for the "open-shell single" solution's formation due to bond-stretching is already the second most important at R_e, and its coefficient is the one to grow most rapidly with the bond elongation.

To quantify potential multi-reference effects in At_2 and put them in perspective, we have analyzed the determinantal structure of the 0_g^+ ground-state FS CCSD solution in the TZ-quality basis near equilibrium and compared it with similar results for I_2. In Fig. 4, we give the coefficients above the 10^{-4} threshold of the determinants contributing to the $(2h,\ 0p)$-sector normalized model vector, except for the dominant one. In the range from $R_e - 0.1$ Å to $R_e + 0.2$ Å, such contributions to the At_2 0_g^+ ground state are markedly larger than in I_2. Thus, while viewing the At_2's ground state as mostly single-reference is qualitatively appropriate, a quantitative description of the At–At bond may not be sufficient at the relativistic single-reference CCSD(T) or multi-reference FS CCSD level alone. A definitive analysis of the At_2's ground state would require relativistic CCSDT and FS CCSDT calculations, which are not feasible yet.

Interestingly, the emergence of the At_2 ground state's slight multi-reference features is linked to the spin-orbit interaction, albeit indirectly in some aspects. One of the spin-orbit effects on the At_2 molecule is a noticeable R_e elongation: from 2.817 Å in 1c-CCSD(T) to 2.957 Å in 2c-CCSD(T). The leading determinants' coefficients of the ground-state 2c FS CCSD $(2h, 0p)$ solution change from 0.98900 and –0.10227 at 2.817 Å to 0.98152 and

–0.14828 at 2.957 Å. Furthermore, comparing 1c and 2c FS CCSD $(2h, 0p)$ solutions at 2.957 Å, we find the leading determinants' coefficients 0.99105 and –0.12207 for 1c and 0.98152 and –0.14828 for 2c. Thus, we can say that the spin-orbit effects interfere with electronic correlations and slightly increase the emerging multi-reference features.

All examined XCF approximations reasonably reproduce the reference R_e and ω_e coupled-cluster data. However, the D_e estimates vary wildly. Pure functionals (B88P86, TPSS, and SCAN) and heavily parameterized hybrids (M06-2X and ωB97XD) give the least satisfactory results. The only XCFs that yield "chemically accurate" results are HSE06, PW6B95, and, marginally, PBE0. Refs. 10,13,71 recognize B3LYP as a safe choice of an XCF approximation for the 2c-RDFT description of the At_2 ground state. Our calculations indicate that it underestimates D_e by about 2 kcal/mol. In contrast to observations in Ref. 13, TPSSh is far from a safe choice as it overestimates D_e by almost 0.2 eV, or 5 kcal/mol.

Fig. 2 demonstrates a strong dependence of $\Delta\mathrm{SO}(E_b)$ on the internuclear distance. For the five representative XCFs, the $\Delta\mathrm{SO}(E_b)$ curves are virtually parallel within a 0.1 eV energy window, which is much narrower than the range of 2c-RDFT data range for the E_b profiles. Relative $\Delta\mathrm{SO}(E_b)$ insensitivity to the XCF choice makes RDFT a reliable tool for extracting the energy component responsible for the spin-orbit effects and their interference with electronic correlations. For the composite scheme shown in Fig. 3, we choose $\Delta\mathrm{SO}(E_b)$ evaluated with HSE06 since this XCF approximation yields the best 2c-RDFT approximation of 2c-CCSD(T) data. The addition of the $\Delta\mathrm{SO}(E_b)$ term to 1c-CCSD(T) results closely reproduces the 2c-CCSD(T) energy profile by causing not only a *ca.* 1 eV weakening of the At—At bond and its elongation by almost 0.3 Å. It is worth stressing that the $\Delta\mathrm{SO}(E_b)$ effect on D_e exceeds the D_e value itself, and the inclusion of spin-dependent relativistic effects in the valence shells is critical for a meaningful description of astatine's molecular properties.

Our composite results, while generally consistent with those in the most recent study by Vasiliu *et al.*[12] and only negligibly deviating from their $\omega_e = 116.5\ \mathrm{cm}^{-1}$ and $R_e = 2.986$ Å, differ noticeably from $D_e = 19.7$ kcal/mol, or 0.854 eV.[12] Our CBS-extrapolated 1c-

CCSD(T) results ($R_e = 2.817$ Å, $D_e = 1.909$ eV, or 44.02 kcal/mol) agree with those in Ref.[12] ($R_e = 2.832$ Å, $D_e = 1.907$ eV, or 43.97 kcal/mol) very well. At the Ref.[12]'s 1c-CCSD(T) $R_e = 2.832$ Å, our $\Delta\mathrm{SO}(E_b) = -27.28$ kcal/mol calculated from 1c- and 2c-CCSD(T) CBS-extrapolated data and their $\Delta\mathrm{SO}(E_b) = -26.98$ kcal/mol virtually match as well. However, the authors[12] use $\Delta\mathrm{SO}(E_b) = -24.278$ kcal/mol for the final binding energy. This spin-orbit term is described as the difference between spin-free and full 4c-CCSD(T) D_e values calculated at the respective R_e values, 2.832 and 2.986 Å, in the uncontracted av3z basis. We find this that this value is surprisingly close to our "vertical" $\Delta\mathrm{SO}(E_b) = -23.44$ kcal/mol at 2.986 Å and matches our $\Delta\mathrm{SO}(E_b) = -24.17$ kcal/mol at the 2c-CCSD(T)'s $R_e = 2.957$ Å. The $\Delta\mathrm{SO}(E_b)$ term derived from our 1c- and 2c-CCSD(T) data at the respective R_e values, following the authors' logic, would have been -26.10 kcal/mol. While we do not have access to the raw data from Ref. 12, we hypothesize that the authors may have inadvertently used the "vertical" $\Delta\mathrm{SO}(E_b) = -24.278$ kcal/mol at 2.986 Å instead of the intended difference between D_e values at the respective equilibrium bond lengths, as claimed in their Table 3 description. The difference between the authors' $\Delta\mathrm{SO}(E_b) = -24.278$ and our -26.10 kcal/mol found according to their prescription seems to be the source of the discrepancy.

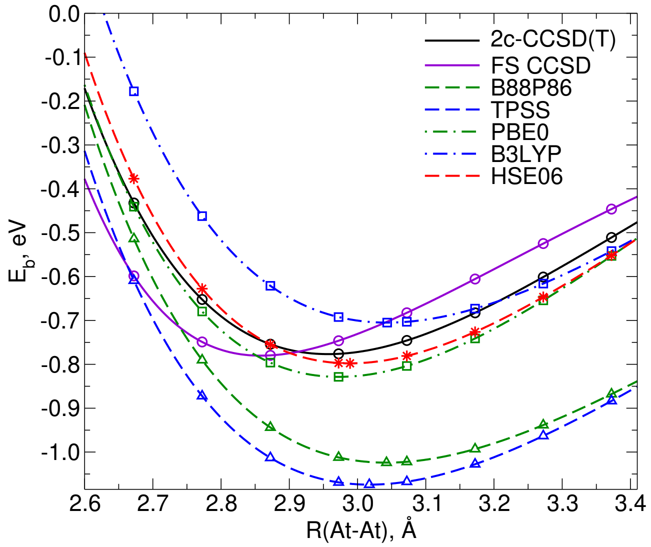

Figure 1: At_2 ground-state binding energy (E_b) profiles obtained using relativistic 2c-CCSD(T) and FS CCSD, and 2c-RDFT approaches.

Table 1: Ground-state properties of the At_2 molecule. This work's coupled-cluster results are extrapolated to the CBS limit.

Method	R_e, Å	D_e, eV	ω_e, cm^{-1}
1c-CCSD(T)	2.817	1.909	162.9
1c-CCSD(T)[12]	2.832	1.907	157.5
2c-CCSD(T)	2.957	0.777	119.4
2c-CCSD(T)[9]	3.006	0.791	110.0
FS CCSD	2.858	0.780	132.1
B88P86	3.042	1.024	106.4
TPSS	3.017	1.074	110.7
SCAN	2.962	1.179	122.7
PBE0	2.972	0.828	120.8
B3LYP	3.043	0.705	108.7
TPSSh	2.995	0.973	115.5
PW6B95	2.989	0.751	116.6
M06-2X	2.935	0.370	129.1
ωB97XD	2.984	0.504	122.5
HSE06	2.989	0.798	117.8
1c-CCSD(T) + ΔSO	2.965	0.792	116.9
1c-CCSD(T) + ΔSO[12]	2.986	0.854	116.5

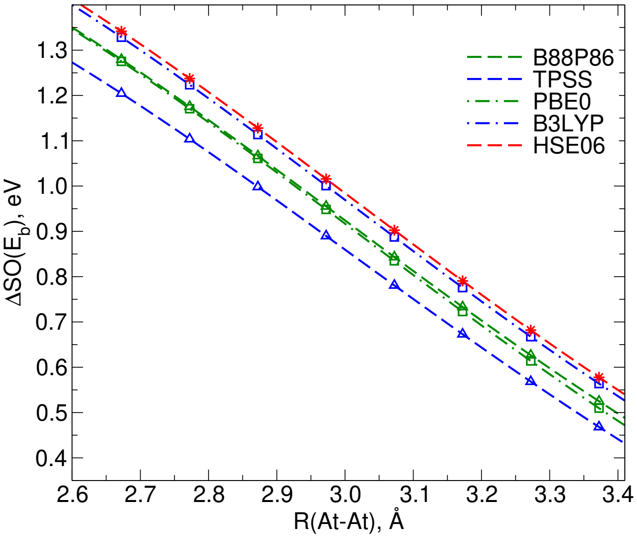

Figure 2: The geometry-dependent ground-state spin-orbit contribution to the binding energy, $\Delta\text{SO}(E_b)$, of At_2 calculated using 1c- and 2c-RDFT with various XCF approximations according to Eq. 2.

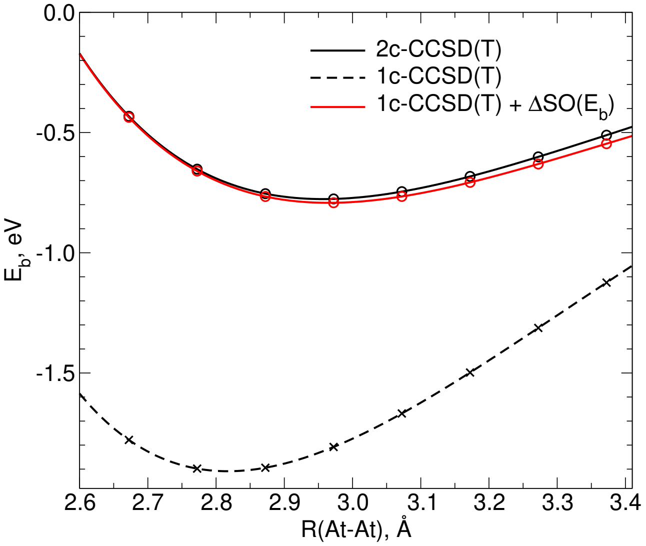

Figure 3: The composite approximation to the 2c-CCSD(T) ground-state E_b profile of At_2 obtained from 1c-CCSD(T) and HSE06 $\Delta SO(E_b)$.

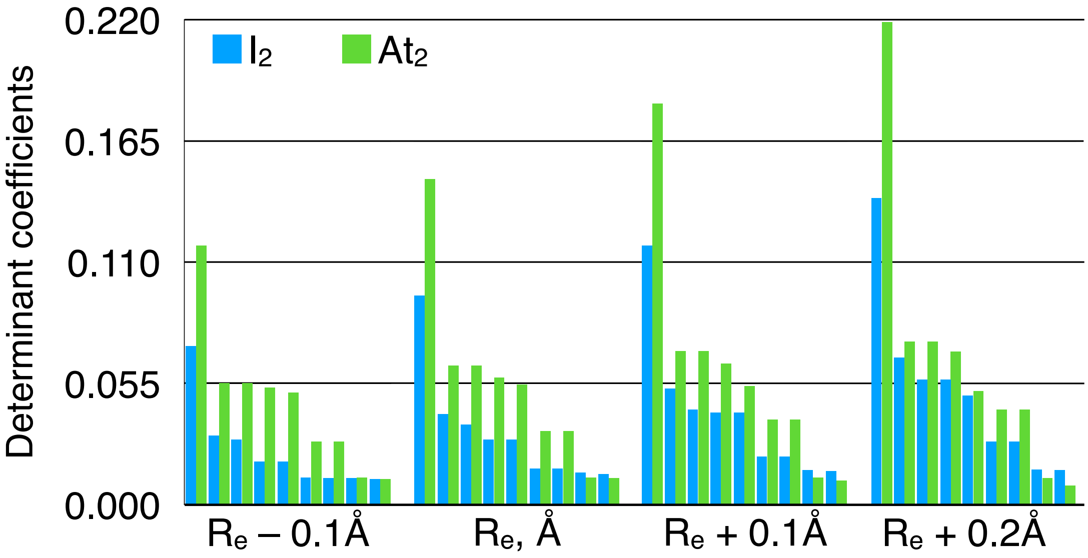

Figure 4: Coefficients of the determinants, excluding the dominant one, that contribute to the $(2h,\ 0p)$-sector FS CCSD solutions for the 0_g^+ ground states of I_2 and At_2. The coefficients are given in the vicinity of the respective R_e values as calculated using the TZ-quality basis sets.

3.2 HAt

Table 2 contains our summary of the HAt ground-state properties, and Figs. 5, 6, and 7 visualize, respectively, E_b profiles, $\Delta\mathrm{SO}(E_b)$ as a function of $R(\mathrm{H—At})$, and the juxtaposition of composite 1c-CCSD(T)+$\Delta\mathrm{SO}(E_b)$ results and 2c-CCSD(T) data. Unlike At_2, HAt has a clear-cut single-reference ground state 0^+ near equilibrium: the FS CCSD solution's dominating determinant has a weight of 0.9999, and the next-largest contribution is only 0.0045. The multi-reference FS CCSD solution accounts for some dynamical-correlation effects, which single-reference 2c-CCSD(T) captures more systematically. Our 1c- and 2c-CCSD(T) results (QZ-to-5Z CBS extrapolation) agree perfectly with, respectively, the CBS-extrapolated all-electron scalar and composite CCSD(T) data in Ref. 12. The deviation from earlier findings[11,72] is most likely due to the basis set quality and core-valence correlation effects, as suggested in Ref. 11.

Out of all XCF approximations tried, only B3LYP gives a "chemically accurate" D_e value with respect to 2c-CCSD(T), although PW6B95 and PBE0 deviate by less than 1.4 kcal/mol. Notably, HSE06 already gives a 3.6 kcal/mol error in D_e despite its remarkable accuracy for At_2. At the same time, the HSE06 estimate of the $\Delta\mathrm{SO}(E_b)$ contribution differs from the CCSD(T) one by less than 0.2 kcal/mol, making the 2c-CCSD(T) and 1c-CCSD(T)+$\Delta\mathrm{SO}(E_b)$ binding energy profiles practically indistinguishable, as illustrated in Fig. 7. Although the spin-orbit effect on $D_e(\mathrm{HAt})$ is not as dramatic as in At_2, it still amounts to almost 30% of the resulting binding energy.

3.3 AtAu

The AtAu results are presented in Table 3 and Figs. 8, 9, and 10. As in HAt, the ground state 0^+ in the relativistic FS CCSD approximation is predominantly single-reference with the leading determinant's coefficient of 0.981. However, a substantial number of determinants with coefficients' magnitudes above 10^{-3} indicates a significant role of dynamical correlations beyond the 2c-CCSD level of theory. It suggests 2c-CCSD(T) as a preferred method to

Table 2: Ground-state properties of the HAt molecule. This work's coupled-cluster results are extrapolated to the CBS limit.

Method	R_e, Å	D_e, eV	ω, cm^{-1}
1c-CCSD(T)	1.690	3.186	2169
1c-CCSD(T)[12]	1.692	3.181	2167
2c-CCSD(T)[72]	1.718	2.446	1994
2c-CCSD(T)	1.721	2.462	1990
4c-CCSD(T)[11]	1.739	2.281	1966
FS CCSD	1.728	2.667	1892
B88P86	1.745	2.616	1911
TPSS	1.737	2.619	1955
SCAN	1.726	2.588	1988
PBE0	1.724	2.403	2013
B3LYP	1.734	2.426	1960
TPSSh	1.730	2.585	1990
PW6B95	1.723	2.405	2002
M06-2X	1.712	2.194	2046
ωB97XD	1.725	2.335	2019
HSE06	1.727	2.305	2002
1c-CCSD(T) + ΔSO	1.722	2.461	1979
1c-CCSD(T) + ΔSO[12]	1.722	2.485	1997

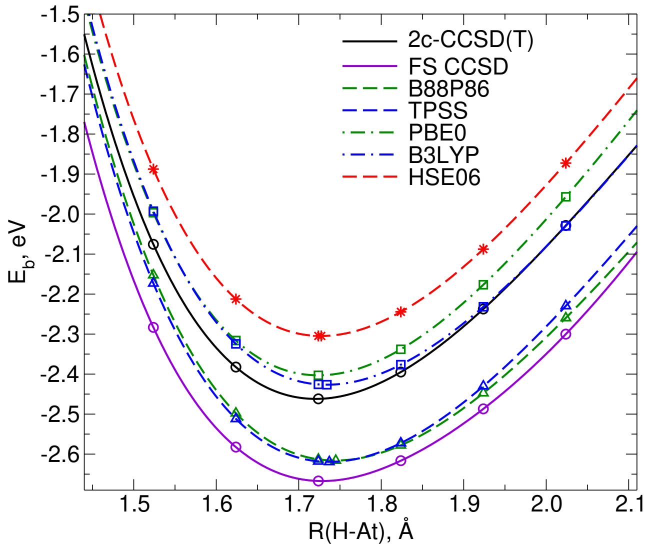

Figure 5: HAt ground-state binding energy (E_b) profiles obtained using relativistic 2c-CCSD(T) and FS CCSD, and 2c-RDFT approaches.

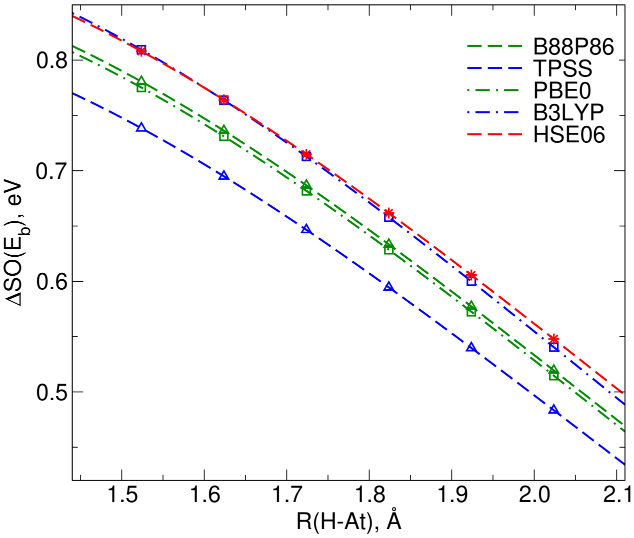

Figure 6: The geometry-depdendent ground-state spin-orbit contribution to the binding energy, $\Delta\mathrm{SO}(\mathrm{E_b})$, of HAt calculated using 1c- and 2c-RDFT with various XCF approximations according to Eq. 2.

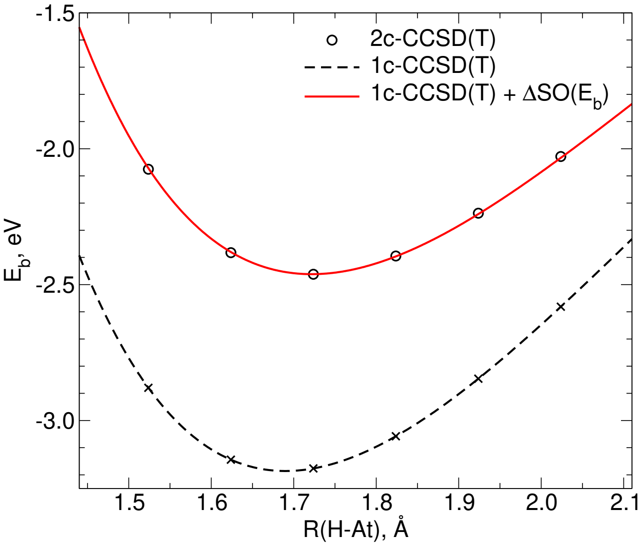

Figure 7: The composite approximation to the 2c-CCSD(T) ground-state E_b profile of HAt obtained from 1c-CCSD(T) and HSE06 $\Delta\mathrm{SO}(\mathrm{E_b})$.

describe the ground state of AtAu.

The only 2c-RDFT calculation that approaches "chemical accuracy" in reproducing the 2c-CCSD(T) D_e value employs TPSSh. PBE0, B88P86, TPSS, and HSE06 yield only marginally acceptable results, while other XCF approximations behave unsatisfactorily. Additionally, we find M06-2X calculations too problematic to converge with either 2c-RDFT implementation and do not present any data for this XCF.

Considering At_2, HAt, and AtAu, it is problematic to pinpoint a single XCF approximation that makes 2c-RDFT and 2c-CCSD(T) data universally consistent. A mostly non-empirical PBE0 approximation demonstrates an overall acceptable behavior in all three cases. However, the extrapolation of the agreement between 2c-RDFT/PBE0 and 2c-CCSD(T) results for diatomic molecules onto more complex structures requires caution.[54,73] The range-separated HSE06 approximation, as in the At_2 and HAt cases, yields the $\Delta SO(E_b)$ estimate closest to CCSD(T), resulting in an overall reasonable agreement between 2c-CCSD(T) and 1c-CCSD(T)+$\Delta SO(E_b)$ results.

Table 3: Ground-state properties of the AtAu molecule. This work's coupled-cluster results are extrapolated to the CBS limit.

Method	R_e, Å	D_e, eV	ω, cm^{-1}
1c-CCSD(T)	2.544	2.572	186.3
2c-CCSD(T)	2.577	1.926	168.7
FS CCSD	2.563	2.013	179.3
B88P86	2.630	2.002	151.4
TPSS	2.617	2.007	155.6
SCAN	2.566	2.207	169.7
PBE0	2.609	1.853	159.1
B3LYP	2.650	1.663	147.9
TPSSh	2.611	1.970	158.0
PW6B95	2.617	1.794	156.1
ωB97XD	2.627	1.676	156.3
HSE06	2.619	1.840	156.7
1c-CCSD(T) + ΔSO	2.580	1.983	167.3

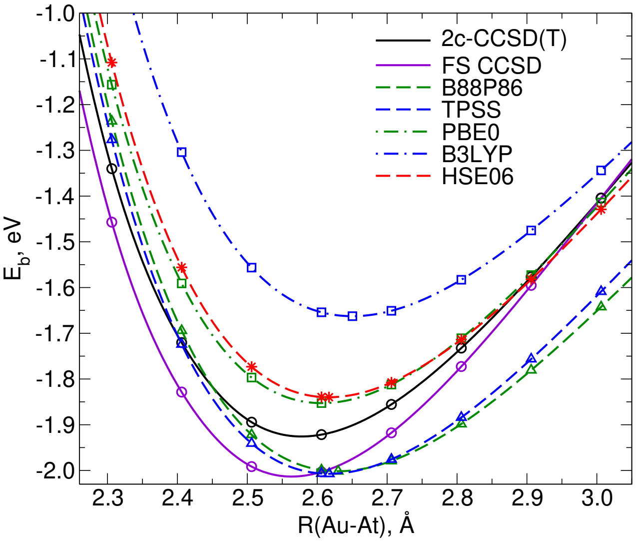

Figure 8: AtAu ground-state binding energy (E_b) profiles obtained using relativistic 2c-CCSD(T) and FS CCSD, and 2c-RDFT approaches.

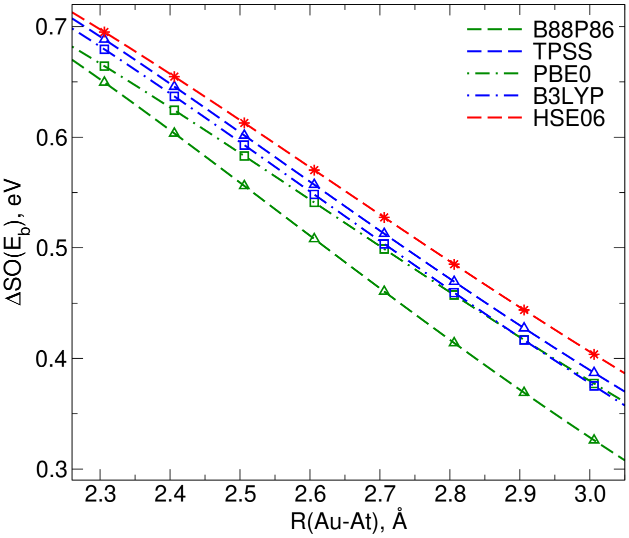

Figure 9: The geometry-dependent ground-state spin-orbit contribution to the binding energy, $\Delta\mathrm{SO}(\mathrm{E_b})$, of AtAu calculated using 1c- and 2c-RDFT with various XCF approximations according to Eq. 2.

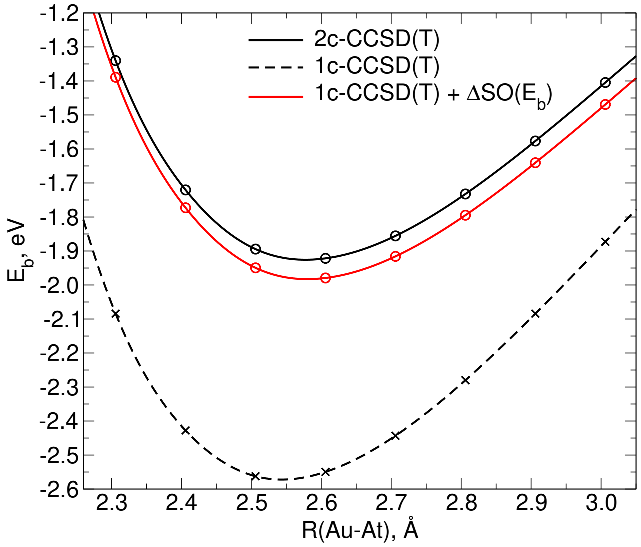

Figure 10: The composite approximation to the 2c-CCSD(T) ground-state E_b profile of AtAu obtained from 1c-CCSD(T) and HSE06 ΔSO($\mathrm{E_b}$).

3.4 $\mathrm{AtO^+}$

While $\mathrm{AtO^+}$ is one of the most studied astatine species,[74–78] some of its basic properties, such as D_e in the ground state, remain difficult to model. The most reliable approaches to incorporate dynamical correlation, spin-orbit interaction, and possible multi-reference character employ advanced perturbative techniques (NEVPT2) and spin-orbit configuration interaction.[74,77] Relativistic FS CCSD is also capable of capturing these effects near equilibrium progressing to the $(2h,\ 0p)$ Fock-space sector[74] from the the closed-shell $\mathrm{AtO^-}$ vacuum and using 10 active holes in the non-trivial sectors. Towards dissociation, however, the appropriate closed-shell vacuum state corresponds to $\mathrm{AtO^{3-}}$, and the FS CCSD model of $\mathrm{AtO^+}$ would require access to the $(4h,\ 0p)$ Fock-space sector. Due to the unavailability of such FS CCSD implementations, it is impossible to evaluate D_e at this level of theory.

A feasible alternative to multi-reference approaches is 2c- or 4c-CCSD(T) with a relativistic closed-shell Hartree–Fock solution as the reference determinant for the 0^+ ground state.[74] However, the application of Dirac–Coulomb 4c-CCSD(T) in Refs. 74 and 77 does not allow to estimate D_e due to problems in finding the ground-state CCSD(T) energy of an oxygen atom with the Dirac–Coulomb Hamiltonian. In the RECP model, we treat all 8 oxygen's electrons explicitly, and the oxygen's contribution the oxygen atom's Hamiltonian becomes a non-relativistic Coulomb operator, which allows us to find the ground ^3P state's CCSD and CCSD(T) energies without any issues. These results are summarized in Table 4.

A more fundamental problem with this CCSD(T) approach is the assumption of the ground state's single-reference character. According to Ref. 74, the T_1 diagnostic value at R(At—O) = 2.0 Å is 0.03, consistent with our $T_1 = 0.037$ and $||T_1|| = 0.207$. A reference-invariant T_2 diagnostic[79] gives 0.1726. While universally adopted critical T_2 diagnostic values are not readily available,[80] the examples in Ref. 79 allow us to argue in favor of the departure from a clear-cut single-reference case. The analysis of the $(2h, 0p)$ FS CCSD wavevector's composition supports this observation. Further elongation of R(At—O) to 2.1 Å leads to a steep increase in T_1 to 0.101, $||T_1||$ to 0.571, and T_2 to 0.1924, consistent with the manifestation of the ground state's multi-reference character. In Fig. 11, we illustrate the change in the determinantal composition of the $(2h, 0p)$ FS CCSD wavevector in the vicinity of R_e. Due to these indications of the single-reference CCSD(T) unreliability, we do not continue the 2c-CCSD(T) binding energy profile beyond 2.1 Å. Also, due to the rapid onset of multi-reference effects, we resort to a finer R(At—O) grid with a 0.01 Å increment and the TZ-to-QZ CBS extrapolation scheme to keep the calculations' volume reasonable.

Among the four species studied here, AtO$^+$ is the most difficult case for 2c-RDFT, especially in predicting D_e. Provided that 2c-CCSD(T) yields reliable ground-state spectroscopic constants, only B3LYP reproduces these results accurately, including a deviation in D_e below 1 kcal/mol. The only other marginally acceptable XCF approximations are PBE0 and PW6B95. In Fig. 12, we show the E_b profiles near equilibrium calculated using 2c-CCSD(T) (TZ-to-QZ CBS extrapolation) and 2c-RDFT with B3LYP and PBE0.

Spin-orbit interaction in AtO$^+$ causes it to be a relativistic closed-shell system in its ground state instead of a spin-triplet in the scalar relativistic approximation.[74] Due to this spin-orbit-induced qualitative change in the ground state's electronic structure, the composite 1c-CCSD(T)+ΔSO(E_b) approach is hardly applicable to AtO$^+$.

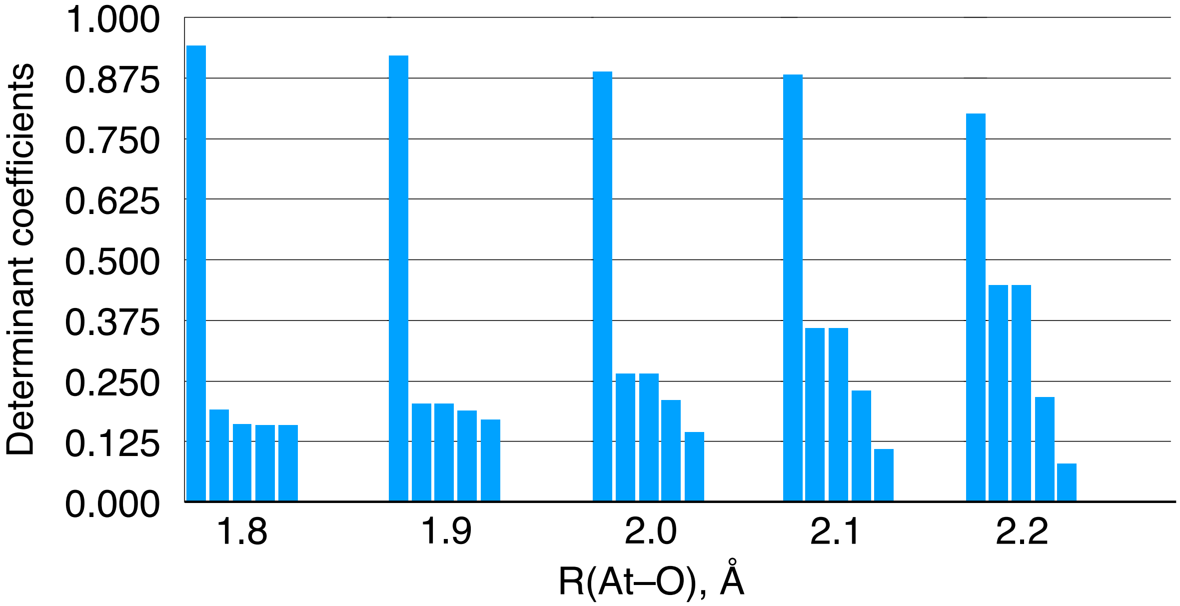

Figure 11: The first five largest coefficients of the determinants, including the dominant one, that contribute to the $(2h,\ 0p)$-sector FS CCSD solution for the 0^+ ground state of AtO^+. These coefficients result from calculations using the TZ-quality basis sets.

Table 4: Ground-state properties of the AtO^+ molecular ion. This work's coupled-cluster results are extrapolated to the CBS limit.

Method	R_e, Å	D_e, eV	ω, cm^{-1}
uc-SOCI/NEVPT2[77]	1.893	2.30	799
4c-CCSD[74]	1.903	—	730
2c-CCSD	1.891	1.664	747.1
4c-CCSD(T)[74]	1.930	—	676
2c-CCSD(T)	1.919	2.320	699.0
B88P86	1.934	3.166	683.0
TPSS	1.930	2.881	688.1
SCAN	1.913	2.619	715.4
PBE0	1.892	2.226	742.6
B3LYP	1.915	2.283	706.4
TPSSh	1.915	2.452	709.9
PW6B95	1.894	2.219	737.0
M06-2X	1.871	1.488	781.1
ωB97XD	1.883	2.044	760.0
HSE06	1.897	2.105	733.8

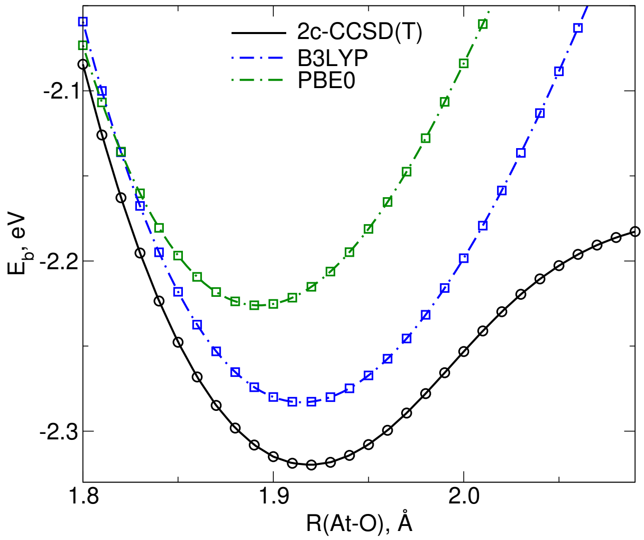

Figure 12: AtO^+ ground-state binding energy (E_b) profiles obtained using relativistic 2c-CCSD(T) and 2c-RDFT approaches.

4 Conclusions

Predictive modeling of astatine compounds' chemical properties poses challenges to high-level *ab initio* and DFT methods. Relativistic CCSD(T) approach in combination with accurate RECPs and bespoke basis sets allows us to provide revised reference data on the ground-state spectroscopic constants of At_2, HAt, AtAu, and AtO^+ via the equal-footing treatment of large relativistic effects, especially spin-orbit interaction, and dynamical electronic correlations. Spin-orbit effects on chemical binding in astatine compounds are critically important: they are responsible for about 30% of binding energy in HAt and AtAu, exceed D_e in At_2, and fundamentally alter the electronic structure of AtO^+. Additionally, it is worth noting that the lack of suitable and generally adopted basis sets for spin-orbit calculations remains an issue for routinely modeling heavy elements' electronic structure and properties.

Relativistic Fock-space CCSD approach reveals some electronic-structure features beyond a typical dynamical-correlation case in At_2 and, in particular, AtO^+. However, modeling the full length of binding-energy curves for At_2 and AtO^+ that would account for spin-orbit, dynamical-correlation, and multi-reference effects remains beyond reach for currently available relativistic coupled-cluster techniques.

Relativistic DFT is indispensable for modeling astatine systems more complex than diatomic molecules. It offers a computationally affordable procedure to simulate spin-free and spin-dependent relativistic and electronic-correlation effects. However, modern relativistic DFT extensions rely on XCF approximations derived or parameterized for non-relativistic systems, which often compromises the results' quality. The combination of non-relativistic XCF approximations with common basis set families compounds such simulations' errors even further. We disentangle these error sources using modified and extended UGBSs and reaching the complete basis set limit. For At_2, HAt, AtAu, and AtO^+, it appears problematic to indicate XCF approximations that would behave consistently well in reproducing *ab initio* coupled-cluster data, PBE0 being a marginal exception, likely owing to its mostly non-empirical character. Empirically fitted XCF tend to behave least satisfactorily. Spin-orbit effects on molecular properties evaluated using relativistic DFT are less sensitive to the XCF choice, which allows for acceptable composite schemes based on scalar-relativistic coupled cluster and spin-orbit DFT approaches. These observations concerning relativistic DFT urge the development of XCF approximations and basis sets suitable for heavy-element molecular systems with large relativistic effects, especially spin-orbit interaction.

Acknowledgement

A.A.R. thanks Drs. Andréi Zaitsevskii and Alexander Oleynichenko for early access to the EXP-T code and technical advice, and Profs. Alexei Kananenka and Michael R. Zalutsky for enlightening discussions. We also thank the Oakland University Technological Services for computing support. Calculations have been performed on the Oakland University high-performance cluster MATILDA. This work is partially supported by the Oakland University Research Committee faculty grant (Summer, 2022).

Supporting Information Available

Technical details on converging two-component Hartree–Fock calculations; all in-house basis sets.

References

(1) Wilbur, D. S. Enigmatic astatine. *Nature Chem.* **2013**, *5*, 246.

(2) Lemonick, S. Astatine is a chemistry puzzle that shows anticancer promise. `https://cen.acs.org/physical-chemistry/Astatine-chemistry-puzzle-shows-anticancer/98/i31`, (accessed November 4, 2022).

(3) Lindegren, S.; Albertsson, P.; Bäck, T.; Jensen, H.; Palm, S.; Aneheim, E. Realizing Clinical Trials with Astatine-211: The Chemistry Infrastructure. *Cancer Biother. Radiopharm.* **2020**, 425–436.

(4) Li, F.; Yang, Y.; Liao, J.; Liu, N. Recent progress of astatine-211 in endoradiotherapy: Great advances from fundamental properties to targeted radiopharmaceuticals. *Chin. Chem. Lett.* **2022**, *33*, 3325–3338.

(5) Guérard, F.; Maingueneau, C.; Liu, L.; Eychenne, R.; Gestin, J.-F.; Montavon, G.; Galland, N. Advances in the Chemistry of Astatine and Implications for the Development of Radiopharmaceuticals. *Acc. Chem. Res.* **2021**, *54*, 3264–3275.

(6) Mease, R. C.; Kang, C.; Kumar, V.; Ray, S.; Minn, I.; Brummet, M.; Gabrielson, K.; Feng, Y.; Park, A.; Kiess, A.; Sgouros, G.; Vaidyanathan, G.; Zalutsky, M.; Pomper, M. G. An improved 211 At-labeled agent for PSMA-targeted alpha therapy. *J. Nucl. Med.* **2022**, *63*, 259–267.

(7) Aneheim, E.; Palm, S.; Jensen, H.; Ekberg, C.; Albertsson, P.; Lindegren, S. Towards elucidating the radiochemistry of astatine – Behavior in chloroform. *Sci. Rep.* **2019**, *9*, 15900.

(8) Chang, Z.; Li, J.; Dong, C. Ionization Potentials, Electron Affinities, Resonance Excitation Energies, Oscillator Strengths, And Ionic Radii of Element Uus (Z = 117) and Astatine. *J. Phys. Chem. A* **2010**, *114*, 13388–13394.

(9) Höfener, S.; Ahlrichs, R.; Knecht, S.; Visscher, L. Relativistic and Non-Relativistic Electronic Molecular-Structure Calculations for Dimers of 4p-, 5p-, and 6p-Block Elements. *ChemPhysChem* **2012**, *13*, 3952–3957.

(10) Macedo, L. G. M. d.; Neves, E. R.; Só, Y. A. d. O.; Gargano, R. Relativistic four-component potential energy curves for the lowest 23 covalent states of molecular astatine (At_2). *Spectrochim. Acta A Mol. Biomol. Spectrosc.* **2021**, *245*, 118869.

(11) Visscher, L.; Styszyñski, J.; Nieuwpoort, W. C. Relativistic and correlation effects on molecular properties. II. The hydrogen halides HF, HCl, HBr, HI, and HAt. *J. Chem. Phys.* **1996**, *105*, 1987–1994.

(12) Vasiliu, M.; Peterson, K. A.; Dixon, D. A. Bond Dissociation Energies in Heavy Element Chalcogen and Halogen Small Molecules. *J. Phys. Chem. A* **2021**, *125*, 1892–1902.

(13) Sergentu, D.; David, G.; Montavon, G.; Maurice, R.; Galland, N. Scrutinizing "Invisible" astatine: A challenge for modern density functionals. *Journal of Computational Chemistry* **2016**, *37*, 1345–1354.

(14) Stephens, P. J.; Devlin, F. J.; Chabalowski, C. F.; Frisch, M. J. Ab Initio Calculation of Vibrational Absorption and Circular Dichroism Spectra Using Density Functional Force Fields. *J. Phys. Chem.* **1994**, *98*, 11623–11627.

(15) Adamo, C.; Barone, V. Toward reliable density functional methods without adjustable parameters: The PBE0 model. *J. Chem. Phys.* **1999**, *110*, 6158–6170.

(16) Ernzerhof, M.; Scuseria, G. E. Assessment of the Perdew–Burke–Ernzerhof exchange-correlation functional. *J. Chem. Phys.* **1999**, *110*, 5029–5036.

(17) Heyd, J.; Scuseria, G. E.; Ernzerhof, M. Hybrid functionals based on a screened Coulomb potential. *J. Chem. Phys.* **2003**, *118*, 8207–8215.

(18) Heyd, J.; Scuseria, G. E.; Ernzerhof, M. Erratum: "Hybrid functionals based on a screened Coulomb potential" [J. Chem. Phys. 118, 8207 (2003)]. *J. Chem. Phys.* **2006**, *124*, 219906.

(19) Krukau, A. V.; Vydrov, O. A.; Izmaylov, A. F.; Scuseria, G. E. Influence of the exchange screening parameter on the performance of screened hybrid functionals. *J. Chem. Phys.* **2006**, *125*, 224106.

(20) Aebersold, L. E.; Wilson, A. K. Considering Density Functional Approaches for Actinide Species: The An66 Molecule Set. *J. Phys. Chem. A* **2021**, *125*, 7029–7037.

(21) Ostrowski, S.; Majkowska-Pilip, A.; Bilewicz, A.; Dobrowolski, J. C. On Au n At clusters as potential astatine carriers. *RSC Adv.* **2017**, *7*, 35854–35857.

(22) Liu, Y.; Zhou, Z.; Feng, Y.; Zhao, X.-G.; Vaidyanathan, G.; Zalutsky, M. R.; Vo-Dinh, T. Gold Nanostars: A Novel Platform for Developing ^{211}At-Labeled Agents for Targeted Alpha-Particle Therapy. *Int. J. Nanomedicine* **2021**, *16*, 7297–7305.

(23) Demidov, Y.; Zaitsevskii, A. A comparative study of molecular hydroxides of element 113 (I) and its possible analogs: Ab initio electronic structure calculations. *Chem. Phys. Lett.* **2015**, *638*, 21–24.

(24) Demidov, Y.; Zaitsevskii, A. Adsorption of the astatine species on a gold surface: A relativistic density functional theory study. *Chem. Phys. Lett.* **2018**, *691*, 126–130.

(25) Burns, J. D.; Tereshatov, E. E.; McCarthy, M. A.; McIntosh, L. A.; Tabacaru, G. C.; Yang, X.; Hall, M. B.; Yennello, S. J. Astatine partitioning between nitric acid and conventional solvents: indication of covalency in ketone complexation of AtO^+. *Chem. Commun.* **2020**, *56*, 9004–9007.

(26) Burns, J. D.; Tereshatov, E. E.; Zhang, B.; Tabacaru, G. C.; McIntosh, L. A.; Schultz, S. J.; McCann, L. A.; Harvey, B. M.; Hannaman, A.; Lofton, K. N.; Sorensen, M. Q.; Haar, A. L. V.; Hall, M. B.; Yennello, S. J. Complexation of Astatine(III) with Ketones: Roles of NO_3^- Counterion and Exploration of Possible Binding Modes. *Inorg. Chem.* **2022**, *61*, 12087–12096.

(27) Mosyagin, N.; Zaitsevskii, A.; Titov, A. Shape-consistent relativistic effective potentials of small atomic cores. *International Review of Atomic and Molecular Physics* **2010**, *1*, 63–72.

(28) Petersburg Nuclear Physics Institute, Quantum Chemistry Laboratory, Effective potentials and basis sets. `http://www.qchem.pnpi.spb.ru/recp`, (accessed November 4, 2022).

(29) Peterson, K. A.; Figgen, D.; Goll, E.; Stoll, H.; Dolg, M. Systematically convergent basis sets with relativistic pseudopotentials. II. Small-core pseudopotentials and correlation consistent basis sets for the post- d group 16–18 elements. *J. Chem. Phys.* **2003**, *119*, 11113–11123.

(30) Figgen, D.; Rauhut, G.; Dolg, M.; Stoll, H. Energy-consistent pseudopotentials for group 11 and 12 atoms: adjustment to multi-configuration Dirac-Hartree-Fock data. *J. Chem. Phys.* **2005**, *311*, 227–244.

(31) Peterson, K. A.; Puzzarini, C. Systematically convergent basis sets for transition metals. II. Pseudopotential-based correlation consistent basis sets for the group 11 (Cu, Ag, Au) and 12 (Zn, Cd, Hg) elements. *Theor. Chem. Acc.* **2005**, *114*, 283–296.

(32) Peterson, K. A.; Yousaf, K. E. Molecular core-valence correlation effects involving the post-d elements Ga-Rn: Benchmarks and new pseudopotential-based correlation consistent basis sets. *J. Chem. Phys.* **2010**, *133*, 174116.

(33) Armbruster, M. K.; Klopper, W.; Weigend, F. Basis-set extensions for two-component spin–orbit treatments of heavy elements. *Phys. Chem. Chem. Phys.* **2006**, *8*, 4862–4865.

(34) Pollak, P.; Weigend, F. Segmented Contracted Error-Consistent Basis Sets of Double- and Triple- Valence Quality for One- and Two-Component Relativistic All-Electron Calculations. *J. Chem. Theory Comput.* **2017**, *13*, 3696–3705.

(35) Franzke, Y. J.; Spiske, L.; Pollak, P.; Weigend, F. Segmented Contracted Error-Consistent Basis Sets of Quadruple- Valence Quality for One- and Two-Component Relativistic All-Electron Calculations. *J. Chem. Theory Comput.* **2020**, *16*, 5658–5674.

(36) DIRAC, a relativistic ab initio electronic structure program, Release DIRAC19 (2019), written by A. S. P. Gomes, T. Saue, L. Visscher, H. J. Aa. Jensen, and R. Bast, with contributions from I. A. Aucar, V. Bakken, K. G. Dyall, S. Dubillard, U. Ekström, E. Eliav, T. Enevoldsen, E. Faßhauer, T. Fleig, O. Fossgaard, L. Halbert, E. D. Hedegård, B. Heimlich–Paris, T. Helgaker, J. Henriksson, M. Iliaš, Ch. R. Jacob, S. Knecht, S. Komorovský, O. Kullie, J. K. Lærdahl, C. V. Larsen, Y. S. Lee, H. S. Nataraj, M. K. Nayak, P. Norman, G. Olejniczak, J. Olsen, J. M. H. Olsen, Y. C. Park, J. K. Pedersen, M. Pernpointner, R. di Remigio, K. Ruud, P. Sałek, B. Schimmelpfennig, B. Senjean, A. Shee, J. Sikkema, A. J. Thorvaldsen, J. Thyssen, J. van Stralen, M. L. Vidal, S. Villaume, O. Visser, T. Winther, and S. Yamamoto (available at `http://dx.doi.org/10.5281/zenodo.3572669`, see also `http://www.diracprogram.org`).

(37) Park, Y.-C.; Lim, I. S.; Lee, Y.-S. Two-Component Spin-orbit Effective Core Potential Calculations with an All-electron Relativistic Program DIRAC. *Bull Korean Chem. Soc.* **2012**, *33*, 803–808.

(38) Kraus, P. Extrapolating DFT Toward the Complete Basis Set Limit: Lessons from the PBE Family of Functionals. *J. Chem. Theory Comput.* **2021**, *17*, 5651–5660.

(39) Castro, E. V. R. d.; Jorge, F. E. Accurate universal Gaussian basis set for all atoms of the Periodic Table. *J. Chem. Phys.* **1998**, *108*, 5225–5229.

(40) Dunning, T. H. Gaussian basis sets for use in correlated molecular calculations. I. The atoms boron through neon and hydrogen. *J. Chem. Phys.* **1989**, *90*, 1007–1023.

(41) Kendall, R. A.; Dunning, T. H.; Harrison, R. J. Electron affinities of the first-row atoms revisited. Systematic basis sets and wave functions. *J. Chem. Phys.* **1992**, *96*, 6796–6806.

(42) Woon, D. E.; Dunning, T. H. Gaussian basis sets for use in correlated molecular calculations. IV. Calculation of static electrical response properties. *J. Chem. Phys.* **1994**, *100*, 2975–2988.

(43) Peterson, K. A.; Dunning, T. H. Accurate correlation consistent basis sets for molecular core-valence correlation effects: The second row atoms Al-Ar, and the first row atoms B-Ne revisited. *J. Chem. Phys.* **2002**, *117*, 10548–10560.

(44) Dr. Andréi Zaitsevskii, private communication. See Sec. S1 of Supporting Information.

(45) Oleynichenko, A. V.; Zaitsevskii, A.; Eliav, E. Towards High Performance Relativistic Electronic Structure Modelling: The EXP-T Program Package. *Commun. Comput. Inf. Sci.* **2020**, 375–386.

(46) Petersburg Nuclear Physics Institute, Quantum Chemistry Laboratory, The EXP-T Program System. `http://www.qchem.pnpi.spb.ru/expt`, (accessed November 4, 2022).

(47) Choi, Y. J.; Lee, Y. S. Spin–orbit density functional theory calculations for heavy metal monohydrides. *J. Chem. Phys.* **2003**, *119*, 2014–2019.

(48) Aprà, E.; Bylaska, E. J.; Jong, W. A. d.; Govind, N.; Kowalski, K.; Straatsma, T. P.; Valiev, M.; Dam, H. J. J. v.; Alexeev, Y.; Anchell, J.; Anisimov, V.; Aquino, F. W.; Atta-Fynn, R.; Autschbach, J.; Bauman, N. P.; Becca, J. C.; Bernholdt, D. E.; Bhaskaran-Nair, K.; Bogatko, S.; Borowski, P.; Boschen, J.; Brabec, J.; Bruner, A.; Cauët, E.; Chen, Y.; Chuev, G. N.; Cramer, C. J.; Daily, J.; Deegan, M. J. O.; Dunning, T. H.; Dupuis, M.; Dyall, K. G.; Fann, G. I.; Fischer, S. A.; Fonari, A.; Früchtl, H.; Gagliardi, L.; Garza, J.; Gawande, N.; Ghosh, S.; Glaesemann, K.; Götz, A. W.; Hammond, J.; Helms, V.; Hermes, E. D.; Hirao, K.; Hirata, S.; Jacquelin, M.; Jensen, L.; Johnson, B. G.; Jónsson, H.; Kendall, R. A.; Klemm, M.; Kobayashi, R.; Konkov, V.; Krishnamoorthy, S.; Krishnan, M.; Lin, Z.; Lins, R. D.; Littlefield, R. J.; Logsdail, A. J.; Lopata, K.; Ma, W.; Marenich, A. V.; Campo, J. M. d.; Mejia-Rodriguez, D.; Moore, J. E.; Mullin, J. M.; Nakajima, T.; Nascimento, D. R.; Nichols, J. A.; Nichols, P. J.; Nieplocha, J.; Otero-de-la Roza, A.; Palmer, B.; Panyala, A.; Pirojsirikul, T.; Peng, B.; Peverati, R.; Pittner, J.; Pollack, L.; Richard, R. M.; Sadayappan, P.; Schatz, G. C.; Shelton, W. A.; Silverstein, D. W.; Smith, D. M. A.; Soares, T. A.; Song, D.; Swart, M.; Taylor, H. L.; Thomas, G. S.; Tipparaju, V.; Truhlar, D. G.; Tsemekhman, K.; Voorhis, T. V.; Vázquez-Mayagoitia, ; Verma, P.; Villa, O.; Vishnu, A.; Vogiatzis, K. D.; Wang, D.; Weare, J. H.; Williamson, M. J.; Windus, T. L.; Woliński, K.; Wong, A. T.; Wu, Q.; Yang, C.; Yu, Q.; Zacharias, M.; Zhang, Z.; Zhao, Y.; Harrison, R. J. NWChem: Past, present, and future. *J. Chem. Phys.* **2020**, *152*, 184102.

(49) Mitin, A. V.; Wüllen, C. v. Two-component relativistic density-functional calculations of the dimers of the halogens from bromine through element 117 using effective core potential and all-electron methods. *J. Chem. Phys.* **2006**, *124*, 064305.

(50) Wüllen, C. v. A Quasirelativistic Two-component Density Functional and Hartree-Fock Program. *Z. Phys. Chem.* **2010**, *224*, 413–426.

(51) Baldes, A.; Weigend, F. Efficient two-component self-consistent field procedures and gradients: implementation in TURBOMOLE and application to Au_{20}^{-}. *Mol. Phys.* **2013**, *111*, 2617–2624.

(52) Balasubramani, S. G.; Chen, G. P.; Coriani, S.; Diedenhofen, M.; Frank, M. S.; Franzke, Y. J.; Furche, F.; Grotjahn, R.; Harding, M. E.; Hättig, C.; Hellweg, A.; Helmich-Paris, B.; Holzer, C.; Huniar, U.; Kaupp, M.; Khah, A. M.; Khani, S. K.; Müller, T.; Mack, F.; Nguyen, B. D.; Parker, S. M.; Perlt, E.; Rappoport, D.; Reiter, K.; Roy, S.; Rückert, M.; Schmitz, G.; Sierka, M.; Tapavicza, E.; Tew, D. P.; Wüllen, C. v.; Voora, V. K.; Weigend, F.; Wodyński, A.; Yu, J. M. TURBOMOLE: Modular program suite for ab initio quantum-chemical and condensed-matter simulations. *J. Chem. Phys.* **2020**, *152*, 184107.

(53) Oleynichenko, A.; Zaitsevskii, A.; Romanov, S.; Skripnikov, L. V.; Titov, A. V. Global and local approaches to population analysis: Bonding patterns in superheavy element compounds. *Chem. Phys. Lett.* **2018**, *695*, 63–68.

(54) Zaitsevskii, A.; Titov, A. V.; Rusakov, A. A.; Wüllen, C. v. Ab initio study of element 113–gold interactions. *Chem. Phys. Lett.* **2011**, *508*, 329–331.

(55) Becke, A. D. Density-functional exchange-energy approximation with correct asymptotic behavior. *Phys. Rev. A* **1988**, *38*, 3098–3100.

(56) Perdew, J. P. Density-functional approximation for the correlation energy of the inhomogeneous electron gas. *Phys. Rev. B* **1986**, *33*, 8822–8824.

(57) Perdew, J. P. Erratum: Density-functional approximation for the correlation energy of the inhomogeneous electron gas. *Phys. Rev. B* **1986**, *34*, 7406–7406.

(58) Tao, J.; Perdew, J. P.; Staroverov, V. N.; Scuseria, G. E. Climbing the Density Functional Ladder: Nonempirical Meta–Generalized Gradient Approximation Designed for Molecules and Solids. *Phys. Rev. Lett.* **2003**, *91*, 146401.

(59) Perdew, J. P.; Tao, J.; Staroverov, V. N.; Scuseria, G. E. Meta-generalized gradient approximation: Explanation of a realistic nonempirical density functional. *J. Chem. Phys.* **2004**, *120*, 6898–6911.

(60) Sun, J.; Ruzsinszky, A.; Perdew, J. P. Strongly Constrained and Appropriately Normed Semilocal Density Functional. *Phys. Rev. Lett.* **2015**, *115*, 036402.

(61) Staroverov, V. N.; Scuseria, G. E.; Tao, J.; Perdew, J. P. Comparative assessment of a new nonempirical density functional: Molecules and hydrogen-bonded complexes. *J. Chem. Phys.* **2003**, *119*, 12129–12137.

(62) Zhao, Y.; Truhlar, D. G. Design of Density Functionals That Are Broadly Accurate for Thermochemistry, Thermochemical Kinetics, and Nonbonded Interactions. *J. Phys. Chem. A* **2005**, *109*, 5656–5667.

(63) Zhao, Y.; Truhlar, D. G. The M06 suite of density functionals for main group thermochemistry, thermochemical kinetics, noncovalent interactions, excited states, and transition elements: two new functionals and systematic testing of four M06-class functionals and 12 other functionals. *Theor. Chem. Acc.* **2008**, *120*, 215–241.

(64) Chai, J.-D.; Head-Gordon, M. Long-range corrected hybrid density functionals with damped atom–atom dispersion corrections. *Phys. Chem. Chem. Phys.* **2008**, *10*, 6615–6620.

(65) Vasiliu, M.; Peterson, K. A.; Marshall, M.; Zhu, Z.; Tufekci, B. A.; Bowen, K. H.; Dixon, D. A. Interaction of Th with H0/−/+: Combined Experimental and Theoretical Thermodynamic Properties. *J. Phys. Chem. A* **2022**, *126*, 198–210.

(66) Rusakov, A. A.; Rykova, E.; Scuseria, G. E.; Zaitsevskii, A. Importance of spin-orbit effects on the isomerism profile of Au_3: An ab initio study. *J. Chem. Phys.* **2007**, *127*, 164322.

(67) Zaitsevskii, A.; Titov, A. V. Interaction of copernicium with gold: Assessment of applicability of simple density functional theories. *Int. J. Quantum Chem.* **2013**, *113*, 1772–1774.

(68) Rothe, S.; Andreyev, A. N.; Antalic, S.; Borschevsky, A.; Capponi, L.; Cocolios, T. E.; Witte, H. D.; Eliav, E.; Fedorov, D. V.; Fedosseev, V. N.; Fink, D. A.; Fritzsche, S.; Ghys, L.; Huyse, M.; Imai, N.; Kaldor, U.; Kudryavtsev, Y.; Köster, U.; Lane, J. F. W.; Lassen, J.; Liberati, V.; Lynch, K. M.; Marsh, B. A.; Nishio, K.; Pauwels, D.; Pershina, V.; Popescu, L.; Procter, T. J.; Radulov, D.; Raeder, S.; Rajabali, M. M.; Rapisarda, E.; Rossel, R. E.; Sandhu, K.; Seliverstov, M. D.; Sjödin, A. M.; Bergh, P. V. d.; Duppen, P. V.; Venhart, M.; Wakabayashi, Y.; Wendt, K. D. A. Measurement of the first ionization potential of astatine by laser ionization spectroscopy. *Nat. Commun.* **2013**, *4*, 1835.

(69) Leimbach, D.; Karls, J.; Guo, Y.; Ahmed, R.; Ballof, J.; Bengtsson, L.; Pamies, F. B.; Borschevsky, A.; Chrysalidis, K.; Eliav, E.; Fedorov, D.; Fedosseev, V.; Forstner, O.; Galland, N.; Ruiz, R. F. G.; Granados, C.; Heinke, R.; Johnston, K.; Koszorus, A.; Köster, U.; Kristiansson, M. K.; Liu, Y.; Marsh, B.; Molkanov, P.; Pašteka, L. F.; Ramos, J. P.; Renault, E.; Reponen, M.; Ringvall-Moberg, A.; Rossel, R. E.; Studer, D.; Vernon, A.; Warbinek, J.; Welander, J.; Wendt, K.; Wilkins, S.; Hanstorp, D.; Rothe, S. The electron affinity of astatine. *Nat. Commun.* **2020**, *11*, 3824.

(70) Visscher, L.; Dyall, K. G. Relativistic and correlation effects on molecular properties. I. The dihalogens F_2 , Cl_2 , Br_2 , I_2 , and At_2. *J. Chem. Phys.* **1996**, *104*, 9040–9046.

(71) Champion, J.; Seydou, M.; Sabatié-Gogova, A.; Renault, E.; Montavon, G.; Galland, N. Assessment of an effective quasirelativistic methodology designed to study astatine chemistry in aqueous solution. *Phys. Chem. Chem. Phys.* **2011**, *13*, 14984–14992.

(72) Gomes, A. S. P.; Visscher, L. The influence of core correlation on the spectroscopic constants of HAt. *Chem. Phys. Lett.* **2004**, *399*, 1–6.

(73) Zaitsevskii, A.; Wüllen, C. v.; Titov, A. V. Communications: Adsorption of element 112 on the gold surface: many-body wave function versus density functional theory. *J. Chem. Phys.* **2010**, *132*, 081102.

(74) Gomes, A. S. P.; Réal, F.; Galland, N.; Angeli, C.; Cimiraglia, R.; Vallet, V. Electronic structure investigation of the evanescent AtO^+ ion. *Phys. Chem. Chem. Phys.* **2014**, *16*, 9238–48.

(75) Shee, A.; Saue, T.; Visscher, L.; Gomes, A. S. P. Equation-of-motion coupled-cluster theory based on the 4-component Dirac–Coulomb(–Gaunt) Hamiltonian. Energies for single electron detachment, attachment, and electronically excited states. *J. Chem. Phys.* **2018**, *149*, 174113.

(76) Ayed, T.; Seydou, M.; Réal, F.; Montavon, G.; Galland, N. How Does the Solvation Unveil AtO^+ Reactivity? *J. Phys. Chem. B* **2013**, *117*, 5206–5211.

(77) Maurice, R.; Réal, F.; Gomes, A. S. P.; Vallet, V.; Montavon, G.; Galland, N. Effective bond orders from two-step spin–orbit coupling approaches: The I_2, At_2, IO^+, and AtO^+ case studies. *J. Chem. Phys.* **2015**, *142*, 094305.

(78) Sergentu, D.-C.; Réal, F.; Montavon, G.; Galland, N.; Maurice, R. Unraveling the hydration-induced ground-state change of AtO^+ by relativistic and multiconfigurational wave-function-based methods. *Phys. Chem. Chem. Phys.* **2016**, *18*, 32703–32712.

(79) Coe, J. P.; Paterson, M. J. Investigating Multireference Character and Correlation in Quantum Chemistry. *J. Chem. Theory Comput.* **2015**, *11*, 4189–4196.

(80) Garza, A. J.; Alencar, A. G. S.; Scuseria, G. E. Actinide chemistry using singlet-paired

coupled cluster and its combinations with density functionals. *J. Chem. Phys.* **2015**, *143*, 244106.

TOC Graphic

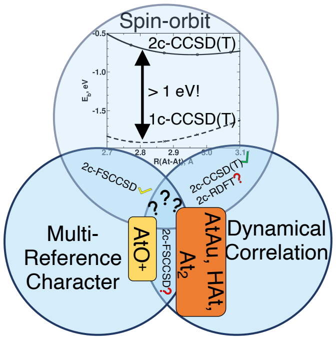
Spin-orbit
-0.5
-1.0
-1.5
E_b, eV
2c-CCSD(T)
> 1 eV!
1c-CCSD(T)
2.7
2.8
2.9
3.0
3.1
R(At-At), Å
2c-FSCCSD ✓
2c-CCSD(T) ✓
2c-RDFT ?
? ? ?
Multi-
Reference
Character
AtO+
2c-FSCCSD ?
AtAu, HAt,
At_2
Dynamical
Correlation